ELECTRONIC PROPERTIES
OF SOLIDS

Electron and Hole Injection
in Metal–Oxide–Nitride–Oxide–Silicon Structures

K. A. Nasyrov[a], S. S. Shaĭmeev[b], V. A. Gritsenko[b], J. H. Han[c], C. W. Kim[c], and J.-W. Lee[c]

[a] Institute of Automatics and Electrometry, Siberian Division, Russian Academy of Sciences,
Novosibirsk, 630090 Russia

[b] Institute of Semiconductor Physics, Siberian Division, Russian Academy of Sciences,
Novosibirsk, 630090 Russia

e-mail: grits@isp.ncs.ru

[c] Samsung Advanced Institute of Technology, P.O. Box 111, Suwon 440-600, Korea

Received June 1, 2005

Abstract—The kinetics of electron and hole accumulation in metal–oxide–nitride–oxide–semiconductor structures is studied. Experimental data are compared with a theoretical model that takes into account tunnel injection, electron and hole capture by traps in amorphous silicon nitride SiN_x, and trap ionization. Agreement between experimental and calculated data is obtained for the band-gap width $E_g = 8.0$ eV of amorphous SiO_2, which corresponds to the barrier for holes $\Phi_h = 3.8$ eV at the Si/SiO_2 interface. The tunneling effective masses for holes in SiO_2 and SiN_x are estimated at $m_h^* \approx (0.4$–$0.5)m_0$. The parameters of electron and hole traps in SiN_x are determined within the phonon-coupled trap model: the optical energy $W_{opt} = 2.6$ eV and the thermal energy $W_T = 1.3$ eV.

PACS numbers: 73.61.Ng, 73.50.Fq, 61.43.–j, and 71.23.An

DOI: 10.1134/S106377610605013X

1. INTRODUCTION

Amorphous dioxide SiO_2 and silicon nitride Si_3N_4 are now two key dielectrics in silicon devices. Because translational symmetry is absent in the amorphous state, band-structure calculations are inapplicable to studying the electronic structure of these important materials. Therefore, these materials are as a rule studied by experimental methods [1, 2]. The band-gap width is a fundamental parameter of an amorphous dielectric. In crystalline semiconductors, this value is determined by band-structure calculations. Depending on whether direct or indirect transitions occur, the spectral dependence of the absorptivity is extrapolated in corresponding coordinates and the band-gap width E_g is determined. The absorptivity in amorphous semiconductors at quantum energies higher than E_g exhibits a power dependence $\alpha(\omega)$ on the quantum energy. It is considered that the dependence $\alpha(\omega)$ is exponential at quantum energies less than E_g (Uhrbach's rule) [3]. At present, there is significant uncertainty in the value of the fundamental parameter, namely, the band-gap width of amorphous SiO_2. According to data of various authors, E_g lies within the range 5.0–10.6 eV [3]. In particular, Mott suggested the value $E_g = 10.6$ eV in the monograph [3].

The rate of electron and hole injection from silicon into the dielectric depends exponentially on the barriers at the Si/SiO_2 interface and on the tunneling effective mass of electrons and holes in SiO_2 and Si_3N_4. The barrier height for electrons at the Si/SiO_2 interface was reliably determined in experiments on internal photoemission to be $\Phi_e = 3.1$ eV [1]. Because the silicon band-gap width equals 1.12 eV, the hole-barrier height at the Si/SiO_2 interface lies in the range $\Phi_h = 0.8$–6.4 eV at values of the SiO_2 band gap equal to 5.0–10.6 eV. Such a large scatter in the hole-barrier height gives rise to a large uncertainty in the predicted hole injection current at the Si/SiO_2 interface, because the latter value depends exponentially on this height. Therefore, a refinement of the band-gap width of amorphous SiO_2 and, hence, the hole-barrier height at the Si/SiO_2 interface is of fundamental importance. The determination of the hole-barrier height at the Si/SiO_2 interface in $Si/SiO_2/Al$ metal–oxide–semiconductor (MOS) structures presents severe problems, because the electron injection rate from Al at a negative potential at Al exceeds the rate of hole injection from Si into SiO_2 by many orders of magnitude.

These problems are overcome when silicon nitride is used in metal–oxide–nitride–oxide–semiconductor (MONOS) structures. The point is that silicon nitride contains a high density ($\approx 10^{19}$–10^{20} cm^{-3}) of electron and hole traps [2] that can capture electron and holes with a giant confinement time (about 10 years at 400 K)
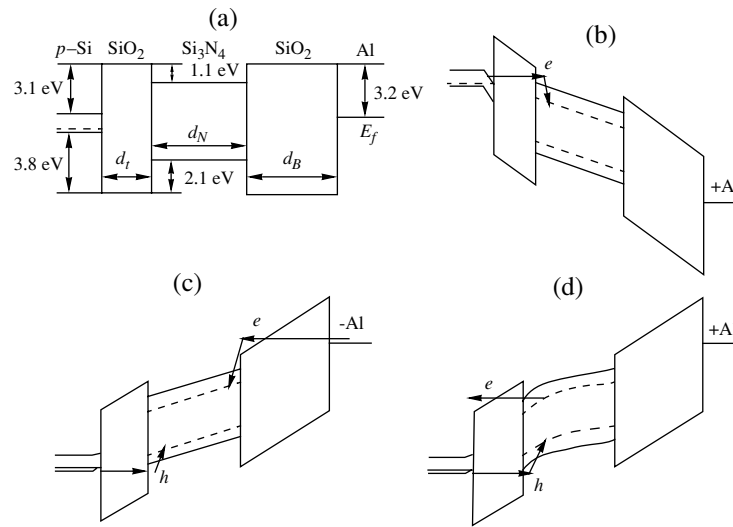
Fig. 1. Energy diagram of a MONOS structure (a) without an applied voltage (flat bands), (b) at a positive potential at the metal (recording), (c) at a negative potential at the metal (erasing), and (d) at a negative potential at the metal for the case when a negative charge is preaccumulated in the nitride (electrons are accumulated).

in the localized state. Therefore, at a negative potential at Al, electrons injected from this contact are captured in silicon nitride, screen the field in the blocking oxide, and, hence, suppress this spurious injection. Moreover, the thickness of the lower tunneling SiO_2 layer in the MONOS structures can be varied, which opens up a possibility in principle for studying hole tunneling from Si through the compound SiO_2/Si_3N_4 barrier (Fig. 1). Thus, the electron- and hole-barrier heights at the Si/SiO_2 interface can be estimated by studying electron and hole injection from silicon in MONOS structures, and, thus, the band-gap width E_g of amorphous SiO_2 can be estimated without using model concepts for the matrix element of electron transition from the valence band to the conduction band due to optical absorption.

Quantum-chemical band-structure calculations of the electronic structure of crystalline SiO_2 [4–6] and Si_3N_4 [7–9] yield an effective electron mass of $m_e^* \approx (0.2–0.6)m_0$ (here, m_0 is the free electron mass). The values of the tunneling effective mass obtained in the majority of experiments on the tunnel injection of electrons into amorphous SiO_2 lie in the range $m_e^* \approx (0.3–0.7)m_0$ [10–14]. However, there are some papers, for example, [15], in which "heavy" electrons ($m_e^* = 3.0m_0$) were observed in amorphous SiO_2.

According to band-structure calculations of the electronic structure of crystalline SiO_2, its valence band consists of two subbands [4–6, 16]. The upper narrow band is formed by nonbonding oxygen $2p_\pi$ orbitals. The narrow band of nonbonding oxygen $2p_\pi$ states is characterized by large values of the effective hole mass $m_h^* \approx (3–10)m_0$ ("heavy" holes) [4, 5]. At the same time, experiments on studying the SiO_2 valence band

by x-ray emission and photoelectron spectroscopy techniques indicate that the top of the SiO_2 valence band is formed not only by nonbonding oxygen $2p_\pi$ orbitals but also by bonding $3s$, $3p$, $3d$ (Si)–$2p$ (O) orbitals [17–19]. The bonding orbitals form a broad valence band, which must be characterized by "light" holes.

A similar situation also occurs in Si_3N_4, in which band-structure calculations predict a large effective hole mass $m_h^* \approx 3m_0$ corresponding to the narrow band of nonbonding nitrogen $2p_\pi$ orbitals [7, 8]. At the same time, there are reports on experimental observations of "light" holes in amorphous Si_3N_4 [20–26].

In this work, electronic processes in MONOS structures are studied with the aim of determining fundamental parameters (band-gap width, barriers, and effective masses) important for the description of electron and hole transfer processes in amorphous silicon dioxide and nitride and also the parameters of traps responsible for the localization of electrons and holes in silicon nitride.

2. SAMPLES AND MEASUREMENT METHODS

P-type silicon with a $\langle 100 \rangle$ orientation doped with boron at a concentration of 5×10^{15} cm^{-3} was used as the substrate. A tunnel nitrided oxide with a thickness of $d_{ox} = 32$ Å was obtained by the thermal oxidation of silicon in dry oxygen at a temperature of 8650°C followed by annealing in N_2O at the same temperature. Amorphous silicon nitride (from here on, silicon-enriched $SiN_{x < 4/3}$ will be designated for simplicity as SiN_x) with a thickness of $d_N = 65$ Å was deposited at
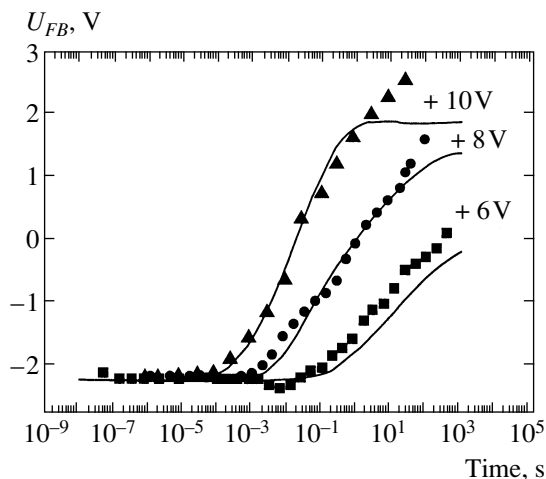
U_{FB}, V

Fig. 2. Negative-charge accumulation in a MONOS structure at a positive gate potential. Points are experiment, and lines are theory. The following parameters were used in the simulation: the barrier for electrons at the Si/SiO$_2$ interface was 3.0 eV, the difference in the electron affinity of SiN$_x$ and SiO$_2$ was 1.1 eV, and effective electron masses were 0.45m_0 in SiO$_2$ and 0.5m_0 in SiN$_x$. The parameters of electron traps in SiN$_x$ were W_{opt} = 2.6 eV, W_T = 1.3 eV, W_{ph} = 0.045 eV, and the trap concentration $N_t = 10^{20}$ cm^{-1}.

730°C from a mixture of dichlorosilane SiH$_2$Cl$_2$ and ammonia in a reduced-pressure reactor at the ratio SiH$_2$Cl$_2$/NH$_3$ = 2.0. The nitride was enriched with excess silicon to increase the concentration of traps responsible for the localization of electrons and holes. Blocking SiO$_2$ with a thickness of d_B = 60 Å was obtained at T = 450°C by oxidizing silane in oxygen in a reduced-pressure reactor at the ratio SiH$_4$/O$_2$ = 5. The thicknesses of three dielectric films used in the MONOS structures were determined by two methods: using laser ellipsometry (λ = 6328 Å) and electron microscopy. The film thicknesses determined by the two methods differed by no more than 2 Å. An aluminum contact with an area of 10^{-4} cm^{-2} obtained by sputtering aluminum in a vacuum followed by photolithography was used as the upper electrode.

The injection of electrons and holes into silicon nitride (data recording and erasing) was performed by applying rectangular pulses of positive and negative polarities, respectively, to the MONOS structures. The kinetics of charge accumulation (erasing) in the nitride was studied by varying the pulse duration in a wide range. The storage properties of the MONOS structures were studied my measuring the flat-band potential (U_{FB}), which was determined from the capacity–voltage (C–V) characteristics measured at a frequency of 100 kHz.

3. EXPERIMENTAL RESULTS

The flat-band potential in the initial structures was $U_{FB} = -2.2$ V, which was caused by the difference in the Fermi energy for Al and the semiconductor substrate and by the occurrence of a positive charge at the Si/SiO$_2$ interface. The existence of this charge leads to the formation of an inversion layer on the entire silicon wafer and, as a consequence, provides a high injection rate of minority charge carriers (electrons) from silicon into the nitride at a positive potential at the metal.

Figure 1 presents an energy band diagram of a MONOS structure in the flat-band regime (a) without an applied voltage and (b–d) at two polarities of the potential at the metal. In the data-recording mode, a positive potential was applied to the metal electrode (Fig. 1b). In this case, electrons are injected from silicon through the tunnel oxide with their subsequent capture by traps in silicon nitride. Negative-charge accumulation leads to a shift of U_{FB} in the positive potential direction. Experimental values of U_{FB} are presented in Fig. 2 (points) as functions of the pulse duration for three values of the pulse amplitude: +6, +8, and +10 V. The dependence of U_{FB} on the pulse duration at long times is close to logarithmic.

In the data erasing mode with the MONOS structures precharged with electrons (U_{FB} = +0.1 V), a negative potential was applied to the metal electrode (see Fig. 1d). Experimental values of U_{FB} are presented in Fig. 3 (points) as functions of the pulse duration for three values of the pulse amplitude: –6, –8, and –10 V. Under the action of a negative pulse, the negative charge in silicon nitride decreases. The change in the value of U_{FB} can be due to (1) the ionization of electron traps in the nitride and the transfer of free electrons to the silicon substrate, (2) the injection of holes from the Si substrate and their capture by hole traps in the nitride, and (3) the injection of holes from the Si substrate and their recombination at electron traps. To describe the experimental results and to determine the parameters of the studied structures, a physical model was developed and a computer program was created for the calculation of processes of charge injection into silicon nitride with regard to the ionization of traps in the nitride by the multiphonon mechanism [25].

4. MODEL

The model consider electron injection from the negatively biased electrode and hole injection from the positively biased electrode. The injection current through the contact was calculated using the modified Fowler–Nordheim mechanism of tunneling from the conduction (valence) band of the semiconductor or the metal into the corresponding band of the nitride. The image forces for electrons and holes were not taken into account. However, injection from the contact through traps in the nitride near the SiO$_2$/SiN$_x$ interface was taken into account.

Charge transfer in the nitride bulk was described by the Shockley–Read–Hall equations and the Poisson equation for the electric field distribution in silicon nitride

$$\frac{\partial n(x,t)}{\partial t} + \frac{\partial n v_n}{\partial x} \tag{1}$$
$$= -\sigma v n(N_t - n_t) + n_t P^{(n)}(x,t) - \sigma_r v n p_t,$$

$$\frac{\partial n_t(x,t)}{\partial t} = \sigma v n(N_t - n_t) - n_t P^{(n)}(x,t) - \sigma_r v p n_t$$
$$+ \mathrm{Inj}^{(n)}(x,t)(N_t - n_t) - \mathrm{Ion}^{(n)}(x,t) n_t, \tag{2}$$

$$\frac{\partial p(x,t)}{\partial t} + \frac{\partial p v_p}{\partial x} \tag{3}$$
$$= -\sigma v p(N_t - p_t) + p_t P^{(p)}(x,t) - \sigma_r v p n_t,$$

$$\frac{\partial p_t(x,t)}{\partial t} = \sigma v p(N_t - n_t) - p_t P^{(p)}(x,t) - \sigma_r v p n_t$$
$$+ \mathrm{Inj}^{(p)}(x,t)(N_t - p_t) - \mathrm{Ion}^{(p)}(x,t) p_t, \tag{4}$$

$$\frac{\partial F}{\partial x} = -e \frac{n_t(x,t) - p_t(x,t)}{\varepsilon \varepsilon_0}. \tag{5}$$

Here, n and n_t are electrons; p and p_t are the concentrations of the free and trapped holes; N_t is the concentration of traps, which in this work is assumed to be equal for electron and hole traps; $F(x, t)$ is the local electric field; e is the electron charge; v_n and v_p are the drift velocities of electrons and holes, respectively; $v = |v_n| = |v_p|$; and $\varepsilon = 7.5$ is the low-frequency dielectric constant of SiN_x. The same capture cross-section σ on traps and the same recombination cross-section σ_r of a free charge carrier with a carrier of the opposite sign localized on a trap were used for electrons and holes. $P^{(n,p)}$ are the probabilities of trap ionization in SiN_x per unit time. $\mathrm{Inj}(x,t)^{(n,p)}$ and $\mathrm{Ion}(x,t)^{(n,p)}$ describe the tunnel injection of charge carriers from the corresponding band of the semiconductor to traps located in the nitride bulk and the reverse process, that is, the ionization of a trap into a band of the semiconductor. To calculate $P^{(n,p)}$, the multiphonon trap ionization model was used [27], in which it is assumed that a trap for an electron or a hole is neutral. An "oscillator" or a "nucleus" embedded in the nitride lattice and capable of attracting and capturing an electron or a hole serves respectively as an electron or hole trap. It is assumed that the energy of a bound electron (hole) depends linearly on the generalized coordinate Q of the "nucleus." Thus, in the course of nucleus vibrations, the energy of the bound electron (hole) varies during the period of nucleus vibrations. In this work, the description of such a trap and its ionization rate fully follows the quantum-mechanical approach developed in the work by Makram-Ebeid and Lannoo [27]. The trap is character-
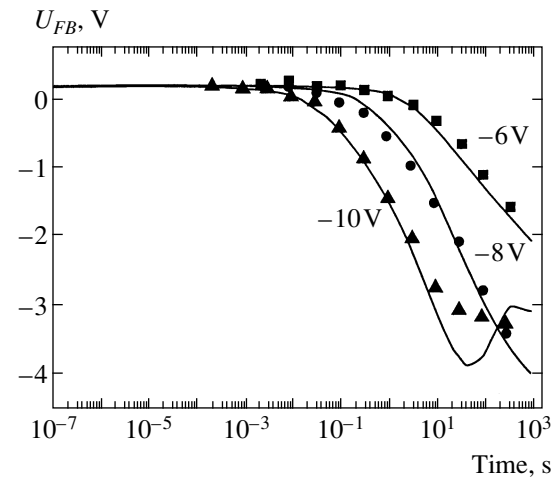

Fig. 3. Kinetics of negative-charge erasing in a MONOS structure at a negative gate potential. Points are experiment, and lines are theory. Traps in the nitride were prefilled with electrons to the value that corresponded to $V_{FB} = 0.1$ eV. The following parameters were used in the simulation. The electron barriers at the Si/SiO_2 and SiN_x/SiO_2 interfaces were 3.0 and 1.1 eV, respectively. The same effective masses were taken for electrons and holes $0.45m_0$ in SiO_2 and $0.5m_0$ in SiN_x. The same parameters were used for electron and hole traps $W_{opt} = 2.6$ eV, $W_T = 1.3$ eV, $W_{ph} = 0.045$ eV, and the trap concentration $N_t = 10^{20}$ cm^{-1}.
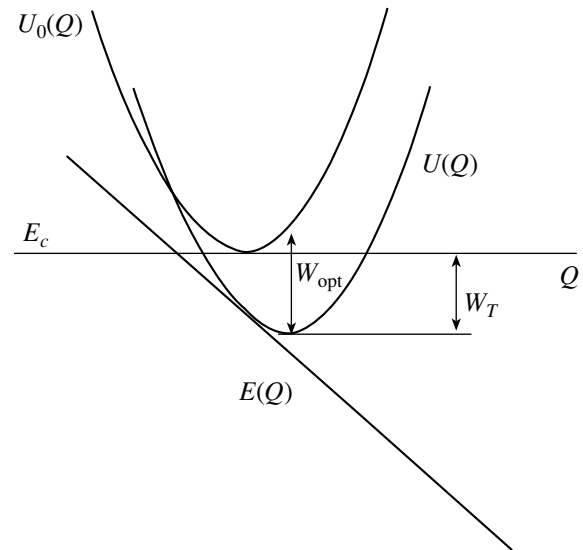

Fig. 4. Configuration diagrams for empty $U_0(Q)$ and filled $U(Q)$ traps. $E(Q)$ is the dependence of the energy level of a trapped electron on the "nucleus" position.

ized by the thermal W_T and optical W_{opt} ionization energies (Fig. 4) and by the phonon energy $W_{ph} = \hbar\omega$, where ω is the nucleus vibration frequency. The external electric field can assist the process of trap ionization. Ionization results in an empty nucleus and a free carrier, whose total energy equals the initial energy of the filled

trap. As a rule, after trap ionization, the nucleus energy corresponds to an excited vibrational state. The excess energy is spent for the excitation of other vibrational modes of the lattice. According to the quantum approach outlined in [27], the following equation is obtained for the trap ionization rate in an external field:

$$P = \sum_{n=-\infty}^{+\infty} \exp\left[\frac{nW_{\mathrm{ph}}}{2kT} - S\coth\frac{nW_{\mathrm{ph}}}{2kT}\right]$$

$$\times I_n\left(\frac{S}{\sinh(W_{\mathrm{ph}}/2kT)}\right)P_i(W_T + nW_{\mathrm{ph}}),$$

$$P_i(W) = \frac{eF}{2\sqrt{2m^*W}}\exp\left(-\frac{4}{3}\frac{\sqrt{2m}}{\hbar eF}W^{3/2}\right), \tag{6}$$

$$S = \frac{W_{\mathrm{opt}} - W_T}{W_{\mathrm{opt}}}.$$

Here, I_n is the modified Bessel function, and $P_i(W)$ describes the probability of charge carrier tunneling from a trap with a short-range potential with the level depth W [28].

In addition, Eqs. (2) and (4) contain terms that describe the tunnel injection of charge carriers from the corresponding band of the semiconductor to traps located in the nitride bulk and the reverse process, that is, the ionization of a trap into a band of the semiconductor. For the first time, this injection mechanism was considered in works by Svensson et al. [29, 30], where injection to multilevel traps and their ionization in the reverse direction were studied. In this work, we generalize this approach to the case of a phonon-coupled trap. In particular, the ionization rate of electrons from the trap to the conduction band of the semiconductor is described by the equation (compare with Eq. (6))

$$\mathrm{Ion}(x) = \sum_n \exp\left[\frac{nW_{\mathrm{ph}}}{2kT} - S\coth\frac{nW_{\mathrm{ph}}}{2kT}\right]$$

$$\times I_n\left(\frac{S}{\sinh(W_{\mathrm{ph}}/2kT)}\right)P_i(W_T + nW_{\mathrm{ph}}),$$

$$\Gamma(W) = \frac{v_{\mathrm{out}}}{2(d_{\mathrm{ox}} + x)}\frac{T(x)}{\left(1 + \left(\frac{m_N^*}{m_S^*} - 1\right)\frac{W}{\Phi_1}\right)^2} \tag{7}$$

$$\times\left(1 - \frac{1}{1 + e^{(E - E_F)/kT}}\right).$$

Here, W is the energy depth of the trap from which tunneling occurs, m_N^* and m_S^* are respectively the effective electron masses in the nitride and the semiconduc-

tor, $T(x)$ is the tunnel transparency of the compound barrier $\mathrm{SiN}_x/\mathrm{SiO}_2$, d_{ox} is the thickness of SiO_2, x is the distance from the trap to the $\mathrm{Si_3N_4}/\mathrm{SiO_2}$ interface, E_F is the Fermi energy in the semiconductor, and v_{out} is the electron velocity in the conduction band of the semiconductor with an energy E equal to the electron energy in the trap. Thus, E and W are related by the equation

$$E = \Phi_1 - \Phi_2 - W - eV(x),$$

where $V(x)$ is the potential at the point x of trap location in the nitride, and Φ_1 and Φ_2 are respectively barrier heights at the $\mathrm{Si}/\mathrm{SiO_2}$ and $\mathrm{SiN}_x/\mathrm{SiO_2}$ interfaces. We assume that the semiconductor substrate is at a zero potential. Thus, $V(x)$ is summed from the voltage drops across the semiconductor, the lower silicon oxide, and the section between the $\mathrm{SiN}_x/\mathrm{SiO_2}$ interface and the point x. Summing over n in Eq. (7) is carried out within the limits for which the value of E is higher than the bottom of the conduction band of the semiconductor near the interface with $\mathrm{SiO_2}$.

The coefficient of electron injection to traps $\mathrm{Inj}(x)$ can be found from the notion that traps in an equilibrium state must be filled in accordance with the Fermi statistics

$$n_t(x) = \frac{N_t}{1 + \exp\left(\dfrac{\Phi_1 - \Phi_2 - W_T - eV(x) - E_F}{kT}\right)}.$$

From stationary Eq. (2), this condition leads to the relationship

$$\mathrm{Inj}(x) = \mathrm{Ion}(x)\exp\left(-\frac{\Phi_1 - \Phi_2 - W_T - eV(x) - E_F}{kT}\right).$$

The coefficients of electron injection to traps and their reverse ionization in the case of holes are calculated quite similarly.

The voltage drop across the semiconductor was found by solving self-consistently the Poisson equation and the charge-carrier distribution in accordance with the Fermi statistics. Quantum size effects associated with the quantization of the carrier spectrum in the inversion layer and the accumulation layer were not taken into account.

5. COMPARISON OF EXPERIMENTAL DATA WITH THEORY

Figure 2 presents the calculated results (solid lines) and experimental data (points) for the case of electron injection from silicon at a positive potential at the metal (see Fig. 1b). The best agreement between the experiment and calculations was obtained at the values of parameters given in the figure caption. From a comparison between the experiment and the calculation, it was
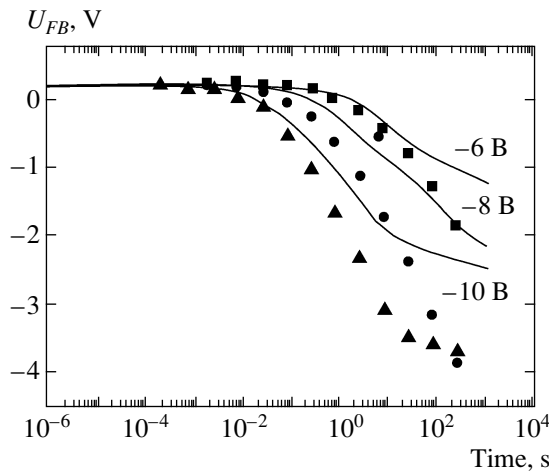
U_{FB}, V

Fig. 5. The same as in Fig. 3 but the calculation was carried out for the case when only ionization of electron traps is allowed and hole injection is blocked.
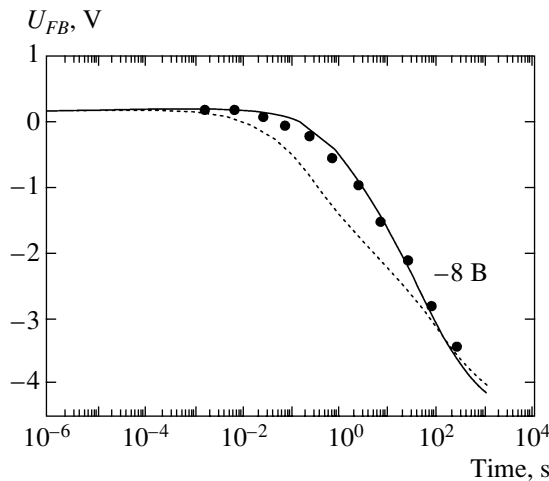
U_{FB}, V

Fig. 6. Experimental dependence of the shift of V_{FB} in the erasing mode (points) for a potential at the metal of –8 V. The solid line is the result of simulation for the trap energy $W_{opt}/W_T = 2.6/1.3$ eV. The dotted line is the result of simulation for the trap energy $W_{opt}/W_T = 2.2/1.1$ eV. The other parameters are the same as in Fig. 3.

found that electron injection at pulse amplitudes of +8 and +10 V occurs from Si to the SiN_x conduction band followed by electron capture by traps in the nitride. At a pulse amplitude of +6 V, injection occurs directly to traps in SiN_x by the multiphonon mechanism. At long times, the calculated dependences $U_{FB}(t)$ exhibit a tendency toward saturation (Fig. 2), which is associated with the ionization of traps in SiN_x followed by electron tunneling through the blocking oxide.

The physical picture of the erasing of the negative charge preaccumulated in Si_3N_4 is more complicated. The calculated results (solid lines) and experimental data (points) are presented in Fig. 3. It is found that the

decrease in the negative charge at relatively small durations of the erasing pulse is associated with the ionization of electron traps in the nitride through back tunneling to the silicon conduction band. Hole injection from the silicon substrate to silicon nitride occurs only at long times. It was suggested in the model that no hole–electron recombination occurred in silicon nitride. Turning off the recombination process does not substantially change the dependence $U_{FB}(t)$. This is due to the fact that the process of negative-charge compensation by positively charged traps results in the same total charge as the recombination of injected holes with electrons localized in SiN_x.

Figure 5 presents the results of calculations that take into account only the ionization of electron traps in SiN_x while hole injection from silicon is blocked. It is evident that the calculated results are in reasonable agreement with the experimental data at short times. However, a significant discrepancy between experiment and theory is observed at long times because of the depletion of traps filled with electrons.

An analysis showed that the dependence $U_{FB}(t)$ in the erasing mode essentially depends on the trap energies at short times. Figure 6 presents the results of modeling the process of negative charge erasing for two different trap energies at –8 V. A decrease in the trap energy to $W_{opt}/W_T = 2.2/1.1$ eV leads to a shift of the calculated dependence $U_{FB}(t)$ toward shorter times as compared with experiment. This phenomenon is explained by the fact that the trap ionization probability increases as the trap energy decreases.

Figure 7 presents the electron emission current from traps and the hole injection current from silicon to the nitride as functions of time for two trap energies. It is evident that the electron ionization current from traps dominates at short times and the hole injection current from silicon dominates at long times. A decrease in the energy of electron traps is accompanied by an increase in the electron ionization current from traps.

To reveal the role of hole injection from silicon at a negative potential at the metal, simulation was performed under conditions when the ionization of electron traps was blocked. In this case, the decrease in the negative charge is due to only the injection of holes from silicon (see Fig. 1d). The ionization of traps was blocked in the calculation by increasing the effective electron mass. Simulation was performed for different values of the hole barrier at the SiO_2/SiN_x interface. The results of simulation are presented in Fig. 8. The best agreement with experiment is achieved when the difference in the hole barrier at the SiN_x/SiO_2 interface equals 2.1 eV, which corresponds to the band-gap width of SiN_x equal to $E_g = 4.8$ eV.

To illustrate the effect of the hole-barrier height at the Si/SiO_2 interface on the tunnel injection of holes from silicon, Figure 9 presents the calculated results for
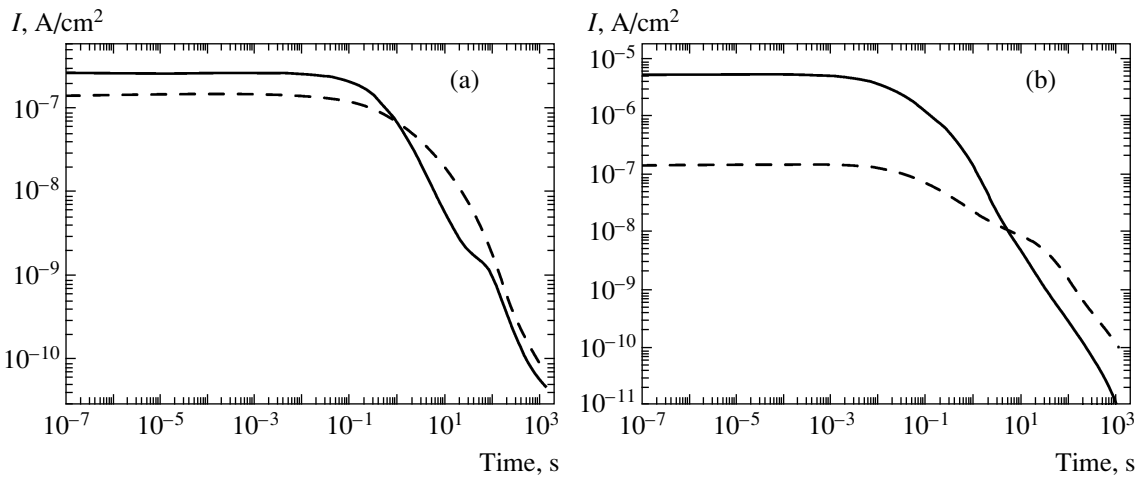
Fig. 7. Results of simulation of the electron (solid line) and hole (dashed line) currents as functions of time through a tunnel oxide for a potential at the metal of –8 V. (a) $W_{opt}/W_T = 2.6/1.3$ eV and (b) $W_{opt}/W_T = 2.2/1.1$ eV. The other parameters are the same as in Fig. 3.

the SiO_2 band-gap width, which is found to be $E_g = 8.7$ eV. The band-gap width 8.7 eV corresponds to the hole-barrier height at the Si/SiO_2 interface equal to $\Phi_h = 4.5$ eV. In this case, the calculated dependences are strongly shifted toward the region of long times as compared with experiment. Agreement with experiment is observed at the SiO_2 band-gap width $E_g = 8.0$ eV, which corresponds to the hole barrier at the Si/SiO_2 interface equal to $\Phi_h = 3.8$ eV. (see Fig. 1a).

Experiments on polarization of the initial (without a charge preaccumulated in the nitride) MONOS structures by a negative potential on the metal (see Fig. 1c) were also performed. Negative-charge accumulation in

SiN_x was observed in an experiment at short times (Fig. 10). It is natural to suggest that the accumulation of electrons in the nitride is associated with their injection from the metal through the blocking SiO_2 layer. If it is suggested that electron injection through the blocking oxide is described by the mechanism of tunneling through a triangular barrier

$$J \propto \exp\left(-\frac{4(2m^*)^{1/2}\Phi^{3/2}}{3\hbar eF}\right), \qquad (8)$$

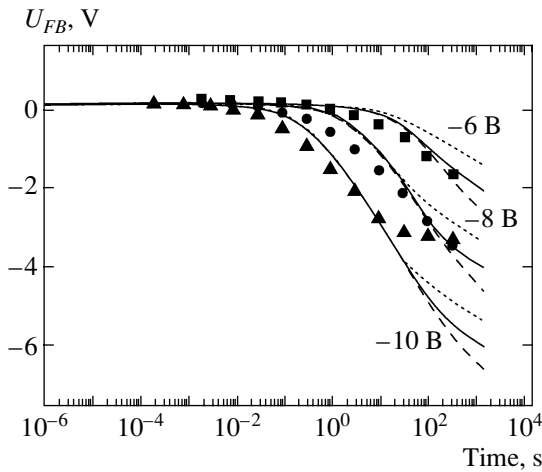then the time τ of the start of an increase in the negative charge (on the U_{FB}–$\ln(t)$ coordinates) is described by

Fig. 8. Results of calculations for the kinetics of negative-charge erasing for various values of hole barriers at the SiN_x/SiO_2 interface: 1.8 eV (dotted lines), 2.1 eV (solid lines), and 2.4 eV (dashed lines). The other parameters are the same as in Fig. 3.
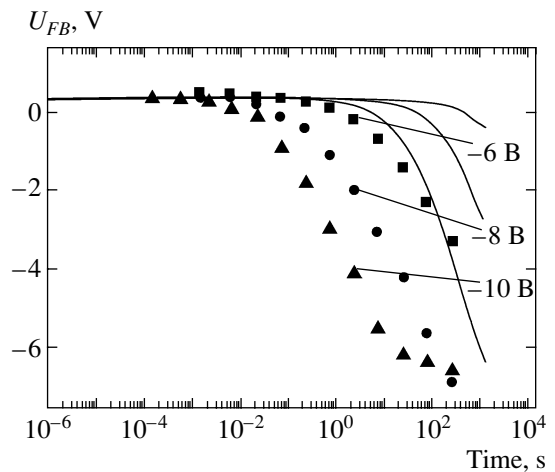

Fig. 9. The same as in Fig. 3, but the calculation is performed for the case when only hole injection is allowed and the ionization of electron traps is blocked. The band-gap width of SiO_2 is 8.7 eV.

the equation

$$\ln(\tau) = \frac{4}{3}\frac{(2m^*)^{1/2}\Phi^{3/2}}{\hbar eF} + C. \qquad (9)$$

From a comparison of $U_{FB}(t)$ plots (Fig. 10) constructed at different applied voltages (or different values of F), the barrier height at the Al/SiO$_2$ interface can be estimated from Eq. (9). At $m_e^* = 0.5m_0$, this height equals $\Phi \approx 1.0$ eV, which is substantially lower than the known barrier for electrons $\Phi = 3.2$ eV at the Al/SiO$_2$ interface [1, 31]. It may be suggested that the blocking oxide most likely contains a great number of traps, through which electrons from aluminum are actually injected [32, 33]. A more detailed study of this phenomenon is beyond the scope of this work.

6. DISCUSSION OF THE RESULTS

In this work, from experiments on the tunnel injection of electrons from silicon to silicon nitride through a compound SiO$_2$/SiN$_x$ barrier, we obtained tunneling effective masses for electrons in SiO$_2$ and SiN$_x$ in the range $m_e^* \approx (0.4–0.5)m_0$. These data are in good agreement with the results of band-structure calculations and with effective masses determined previously in experiments on electron tunneling in SiO$_2$ and Si$_3$N$_4$ [10–14, 20–26]. At the same time, it was reported in [15] that electrons with an effective mass of $m_e^* = 3.0m_0$ were observed in SiO$_2$. It seems that this result can be due to an incorrect interpretation of the experiment, in particular, the neglect of the possibility of direct electron tunneling from silicon to traps in silicon nitride. On the other hand, the effective masses for electrons and holes obtained for Si$_3$N$_4$ in [34] equal $m_e^* = (0.05–0.13)m_0$ and $m_h^* = 0.005m_0$ (superlight electrons and holes). The latter results can be explained by the neglect of the tunnel-thin SiO$_2$ layer between Si and Si$_3$N$_4$, which increases the probability of the tunnel injection of electrons and holes into the dielectric by several orders of magnitude because of the low dielectric constant of the oxide (enhancement of the field in SiO$_2$).

The tunneling effective masses for holes in SiO$_2$ and SiN$_x$ obtained from our experiments on the tunnel injection of holes from silicon to silicon nitride through the compound SiO$_2$/SiN$_x$ barrier are in the range $m_h^* \approx (0.4–0.5)m_0$. These values are in good agreement with the experimental values determined previously in [12, 20, 21, 35, 36]. However, these data contradict the results of band-structure calculations of crystalline SiO$_2$ and Si$_3$N$_4$, which predict the occurrence of only heavy holes in SiO$_2$ and Si$_3$N$_4$.
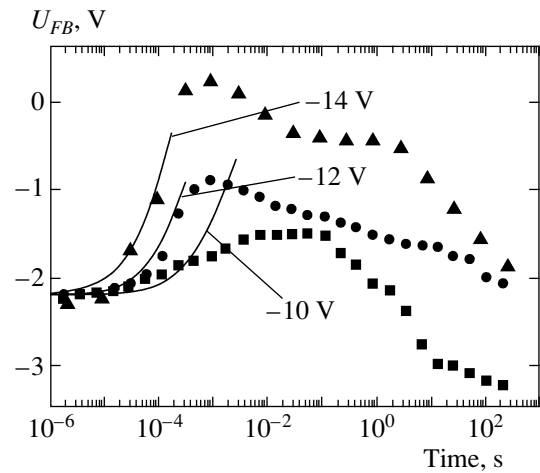

Fig. 10. Charge accumulation kinetics in a nonpolarized MONOS structure at various values of the negative potential at the metal (see Fig. 1c). Points are experiment, and lines are calculated for electron injection by the Fowler–Nordheim mechanism for the barrier $\Phi = 1.0$ eV and a tunneling effective mass of $0.5m_0$.

As was already mentioned above, the band-structure calculations of the electronic structure of SiO$_2$ demonstrate that the top of the valence band is formed by nonbonding oxygen $2p_\pi$ orbitals, which form a narrow band and, hence, yield a large value for the effective hole mass $m_h^* \approx 5m_0$. However, experiments on x-ray emission, photoelectron, and ultraviolet photoelectron spectroscopies indicate that the narrow band of nonbonding oxygen $2p_\pi$ orbitals overlaps by energy in SiO$_2$ with the broad band of bonding silicon $3s$, p, d-0, and $2p$ orbitals. The same result was obtained in quantum-chemical cluster calculations of the electronic structure of SiO$_2$ by both semiempirical [18] and ab initio [19, 37] methods. Unfortunately, cluster calculations give way of determining the effective masses for neither electrons nor holes. Hence, it is of interest to perform refined band-structure calculations for SiO$_2$ with the aim to identify light holes.

Band-structure calculations for Si$_3$N$_4$ also predict an effective hole mass of $m_h^* \approx 3m_0$. At the same time, the tunnel injection of holes in our experiments is adequately described by a tunneling effective mass of $m_h^* \approx 4m_0$. This value agrees with the value $m_h^* \approx (0.4–0.5)m_0$ obtained previously in experiments on the tunnel injection of holes into SiN$_x$. Quantum-chemical cluster calculations of the electronic structure of Si$_3$N$_4$ also point to the occurrence of not only the narrow bond of nonbonding nitrogen $2p$ states but also a broad band of bonding $3s$, p-N, and $2p$ states of silicon [37–40]. This broad band of bonding states must correspond to light holes observed in tunneling experiments. Thus, it is also of interest to perform refined band-structure calculations for Si$_3$N$_4$ with the aim to detect light holes.

Experiments on the determination of the hole-barrier height at the Si/SiO$_2$ interface by x-ray photoelectron spectroscopy (the exciting quantum energy is 1486.6 eV) yield a value of $\Phi_h = 4.3 \pm 0.2$ eV [41]. The value obtained in this work $\Phi_h = 3.8$ eV is by 0.5 eV lower. This discrepancy is explained by the fact that the top of the SiO$_2$ valence band is mainly formed by oxygen 2p orbitals, whereas silicon 3s, p, and d orbitals make a relatively small contribution at the top of the valence band. At the same time, it is the silicon 3s and p orbitals that make the main contribution to the photoionization of valance electrons, because the photoionization cross-section of oxygen 2p orbitals is by an order of magnitude less than the photoionization cross-section of silicon 3s and p electrons [42]. The sensitivity of x-ray photoelectron spectroscopy is not sufficient for the detection of oxygen 2p electrons, which form the top of the valence band. Thus, x-ray photoelectron spectroscopy overestimates the hole-barrier value at the Si/SiO$_2$ interface. The hole barrier $\Phi_h = 3.8$ eV obtained in this work coincides with that obtained previously in [43] by the internal photoemission of holes at the Si/SiO$_2$ interface.

The hole barrier at the Si/SiO$_2$ interface $\Phi_h = 3.8$ eV determined in this work corresponds to the band-gap width of amorphous SiO$_2$ $E_g = 8.0$ eV. This value coincides with the fundamental optical absorption edge and the photoconductivity threshold of amorphous thermal SiO$_2$ oxide on silicon according to the data published in [44, 45]. At the same time, the band-gap width of the thermal oxide on silicon obtained in [46] from the same experiments equals 9.3 eV. In the latter work, it is suggested that the absorption at quantum energies in the range 8.0–9.3 eV is due to the occurrence of "tails in the density of localized states." The notions of "tails in the density of localized states" in amorphous semiconductors and dielectrics are widespread and are discussed in detail, for example, in the books by Mott [3] and Ziman [47]. The band-gap width of SiO$_2$ obtained in this work $E_g = 8.0$ eV indicates most likely that "tails in the density of localized states" are absent in this amorphous dielectric.

The following facts can also be invoked in favor of this statement. The notions of tails of localized states suggests that, in the band gap of SiO$_2$ near the edges of the allowed bands, there are localized states for electrons (near the edge of the conduction band E_c) and for holes (near the edge of the valence band E_v). Given localized states in the forbidden gap near the edge of the conduction band E_c, injected electrons must be captured by localized states (traps), which would lead to a sharp decrease in conductivity because of a decrease in mobility. However, experiments on electron transfer in amorphous SiO$_2$ point to a high mobility of electrons $\mu \approx 20$ cm^2 V^{-1} s^{-1} [48, 49].

Moreover, the absence of localized states for electrons and holes (electron and hole traps) in amorphous SiO$_2$ is confirmed by reprogramming experiments with modern flash (fast) memory transistors. A flash memory element of the first type represents a metal–dielectric–semiconductor (MDS) field-effect transistor in which there is a polysilicon isolated (floating) gate in the gate dielectric [50]. The reprogramming of such a memory element is carried out by means of electron injection from silicon through SiO$_2$ into the floating gate and the back tunneling of electrons from the floating gate into the silicon substrate. If there were localized electron states in SiO$_2$ (electron traps), the reprogramming of flash memory elements would be impossible because of the accumulation of electrons (negative charge) on traps in SiO$_2$.

The absence of localized hole states in SiO$_2$ is evidenced by reprogramming experiments with flash memory transistors of the second type. In this type of flash memory, MONOS structures are used. Silicon nitride serves as memory media, in which electrons and holes are accumulated (localized) on traps [51]. In the reprogramming mode, holes are injected from silicon into silicon nitride through SiO$_2$. If there were hole traps in SiO$_2$, the reprogramming of the second-type flash memory would be impossible because of positive-charge accumulation on traps in SiO$_2$. Thus, the absence of the capture of electrons and holes indicate that there are no tails of localized states in SiO$_2$.

The problem of "tails in the density of states" in amorphous Si$_3$N$_4$ was discussed in detail by one of the authors of this work in [52]. Based on an analysis of experimental data, the inference was made about the absence of "tails in the density of states" in amorphous Si$_3$N$_4$.

In this work, values of optical $W_{opt} = 2.6$ eV and thermal $W_T = 1.3$ eV trap energies were obtained within the framework of the multiphonon ionization theory. These values are lower than the values $W_{opt} = 3.0$ eV and $W_T = 1.5$ eV found previously in experiments on electron and hole transfer in silicon nitride close in chemical composition to stoichiometric Si$_3$N$_4$ in strong electric fields [25]. This circumstance is related to the fact that electron and hole localization was studied in this work in nonstoichiometric silicon nitride enriched with excess silicon SiN$_{x < 4/3}$. It is known that the enrichment of the nitride with excess silicon is accompanied by a decrease in the energies of electron and hole traps [52]. Thermal trap energies in silicon nitride were found previously from transfer experiments in the range 1.2–1.5 eV [53]. Trap energies in the nitride were found from exoelectron-emission experiments in the range 0.7–1.1 eV [54]. The thermal trap energy obtained in this work 1.3 eV is close to half the Stokes shift 1.4 eV obtained from the luminescence spectrum of SiN$_x$ [55]. The optical trap energy found in this work

$W_{opt} = 2.6$ eV can be compared with the photoionization threshold of traps in silicon nitride, which lies in the range 2.0–3.4 eV [56].

ACKNOWLEDGMENTS

REFERENCES

1. V. A. Gritsenko, *Atomic and Electronic Structure of Amorphous Dielectrics in Silicon MIS Devices* (Nauka, Novosibirsk, 1993), p. 280 [in Russian].

2. V. A. Gritsenko, in *Silicon Nitride in Electronics* (Elsevier, Amsterdam, 1988), p. 263.

3. N. F. Mott and E. A. Davis, *Electronic Processes in Non-Crystalline Materials*, 2nd ed. (Clarendon, Oxford, 1979; Mir, Moscow, 1982), p. 432.

4. P. M. Schneider and W. B. Fowler, Phys. Rev. Lett. **36**, 425 (1976).

5. J. R. Chelikowsky and M. Schluter, Phys. Rev. B **15**, 4020 (1977).

6. E. Gnani, S. Reggiani, R. Colle, et al., IEEE Trans. Electron Devices **47**, 1795 (2000).

7. S.-Y. Ren and W. Y. Ching, Phys. Rev. B **23**, 5454 (1981).

8. Y.-N. Xu and W. Y. Ching, Phys. Rev. B **51**, 17379 (1995).

9. S.-D. Mo, L. Quyang, and W. Y. Ching, Phys. Rev. Lett. **83**, 5046 (1999).

10. M. V. Fischetti, Phys. Rev. Lett. **53**, 1755 (1984).

11. M. V. Fischetti, D. J. DiMaria, L. Dori, et al., Phys. Rev. B **35**, 4404 (1987).

12. W.-C. Lee and C. Hu, IEEE Trans. Electron Devices **48**, 1366 (2001).

13. Y.-C. Yeo, T.-J. King, and C. Hu, Appl. Phys. Lett. **81**, 2091 (2002).

14. A. Roy and M. H. White, Solid-State Electron. **34**, 1083 (1991).

15. S. Horiguchi and H. Yoshino, J. Appl. Phys. **15**, 1597 (1985).

16. E. K. Chang, M. Rohlfing, and S. G. Louie, Phys. Rev. Lett. **85**, 2613 (2000).

17. I. A. Brytov, V. A. Gritsenko, and Yu. N. Romashchenko, Zh. Éksp. Teor. Fiz. **89**, 562 (1985) [Sov. Phys. JETP **62**, 321 (1985)].

18. V. A. Gritsenko, R. M. Ivanov, and Yu. N. Morokov, Zh. Éksp. Teor. Fiz. **108**, 2216 (1995) [JETP **81**, 1208 (1995)].

19. V. A. Gritsenko, Yu. N. Novikov, A. V. Shchaposhnikov, et al., Fiz. Tekh. Poluprovodn. (St. Petersburg) **35**, 1041 (2001) [Semiconductors **35**, 997 (2001)].

20. V. A. Gritsenko and E. E. Meerson, Mikroélektronika **17**, 349 (1988).

21. V. A. Gritsenko, Yu. N. Morokov, and E. E. Meerson, Phys. Rev. B **57**, R2081 (1997).

22. Y. C. Yeo, Q. Lu, W. C. Lee, et al., IEEE Electron Device Lett. **21**, 540 (2000).

23. H. Y. Yu, Y. T. Hou, M. F. Li, et al., IEEE Electron Device Lett. **23**, 285 (2002).

24. K. A. Nasyrov, Yu. N. Novikov, V. A. Gritsenko, et al., Pis'ma Zh. Éksp. Teor. Fiz. **77**, 455 (2003) [JETP Lett. **77**, 385 (2003)].

25. K. A. Nasyrov, V. A. Gritsenko, Yu. N. Novikov, et al., J. Appl. Phys. **96**, 4293 (2004).

26. K. A. Nasyrov, V. A. Gritsenko, M. K. Kim, et al., IEEE Electron Device Lett. **23**, 336 (2002).

27. S. S. Makram-Ebeid and M. Lannoo, Phys. Rev. B **25**, 6406 (1982).

28. L. D. Landau and E. M. Lifshitz, *Course of Theoretical Physics*, Vol. 3: *Quantum Mechanics: Non-Relativistic Theory*, 5th ed. (Fizmatgiz, Moscow, 2002; Oxford Univ. Press, Oxford, 1980).

29. C. Svensson and I. Lundstrom, J. Appl. Phys. **44**, 4657 (1973).

30. L. Lundkvist, I. Lundstrom, and C. Svensson, Solid-State Electron. **16**, 811 (1973).

31. S. M. Sze, *Physics of Semiconductor Devices,* 2nd ed. (Wiley, Taiwan, Taipei, 1985; Mir, Moscow, 1984), p. 868.

32. A. V. Chaplik and M. V. Éntin, Zh. Éksp. Teor. Fiz. **67**, 208 (1974) [Sov. Phys. JETP **40**, 106 (1974)].

33. M. Houssa, M. Tuominen, M. Naili, et al., J. Appl. Phys. **87**, 8615 (2000).

34. P. C. Arnett and D. J. DiMaria, J. Appl. Phys. **47**, 2092 (1976).

35. Y. C. Yeo, Q. Lu, W. C. Lee, et al., IEEE Electron Device Lett. **21**, 540 (2000).

36. H. Iwata, Jpn. J. Appl. Phys., Part 1 **41**, 552 (2002).

37. A. V. Shchaposhnikov, V. A. Gritsenko, G. M. Zhidomirov, et al., Fiz. Tverd. Tela (St. Petersburg) **44**, 985 (2002) [Phys. Solid State **44**, 1028 (2002)].

38. V. A. Gritsenko, Yu. N. Morokov, Yu. N. Novikov, et al., Fiz. Tverd. Tela (St. Petersburg) **39**, 1342 (1997) [Phys. Solid State **39**, 1191 (1997)].

39. V. A. Gritsenko, Yu. N. Morokov, and Yu. N. Novikov, Appl. Surf. Sci. **113/114**, 417 (1997).

40. V. A. Gritsenko, A. V. Shaposhnikov, W. M. Kwok, et al., Thin Solid Films **437**, 135 (2003).

41. V. A. Gritsenko, H. Wong, W. M. Kwok, et al., J. Vac. Sci. Technol. B **21**, 241 (2003).

42. J.-J. Yeh, *Atomic Calculation of Photoionization Cross-Sections and Asymmetry Parameters* (Gordon and Breach, Langhorne, PA, 1993), p. 223.

43. A. M. Goodman, Phys. Rev. **152**, 780 (1966).

44. R. J. Powell and M. Morad, J. Appl. Phys. **49**, 2499 (1978).

45. S. L. Boĭtsov, A. Ya. Vul', A. T. Dideĭkin, et al., Fiz. Tverd. Tela (Leningrad) **33**, 1784 (1991) [Sov. Phys. Solid State **33**, 1003 (1991)].

46. Z. A. Weinberg, G. W. Rubloff, and E. Bassous, Phys. Rev. B **19**, 3107 (1979).

47. J. M. Ziman, *Models of Disorder: The Theoretical Physics of Homogeneously Disordered Systems* (Cambridge Univ. Press, Cambridge, 1979; Mir, Moscow, 1982).

48. A. M. Goodman, Phys. Rev. **164**, 1145 (1967).

49. R. C. Huges, Phys. Rev. Lett. **35**, 449 (1975).

50. J. Ranaweera, W. T. Ng, and C. A. T. Salama, Solid-State Electron. **43**, 263 (1999).

51. I. Bloom, P. Pavan, and B. Eitan, Microelectron. Eng. **59**, 213 (2001).

52. V. A. Gritsenko, in *Silicon Nitride in Electronics* (Nauka, Novosibirsk, 1982), p. 199 [in Russian].

53. V. A. Gritsenko, E. E. Meerson, I. V. Travkov, et al., Mikroélektronika **16**, 42 (1987).

54. G. Rosenman, M. Naich, M. Molotskii, et al., Appl. Phys. Lett. **80**, 2743 (2002).

55. V. A. Gritsenko, D. V. Gritsenko, Yu. N. Novikov, et al., Zh. Éksp. Teor. Fiz. **125**, 868 (2004) [JETP **98**, 760 (2004)].

56. S. B. Bibyk and V. J. Kapoor, J. Appl. Phys. **52**, 7313 (1981).

Translated by A. Bagatur'yants

Spell: ok